metals

MDPI

Article

Acquiring High-Quality Oil Casing Steel 26CrMoVTiB under Optimal Continuous Casting Process Conditions

Yingying Zhai [1,2], Kefeng Pan [2,*] and Dapeng Wu [3]

[1] Computing Center, Northeastern University, Shenyang 110819, China
[2] School of Metallurgy, Northeastern University, Shenyang 110819, China
[3] College of Science, Liaoning Shihua University, Fushun 113001, China
* Correspondence: xiaopandy@126.com; Tel.: +86-130-7063-9976

Received: 6 July 2019; Accepted: 4 September 2019; Published: 9 September 2019

Abstract: While the solidification macrostructure of continuous cast billets is an important factor influencing the final performance and rolling yield of oil casing steel, the continuous casting process parameters have a direct influence on the solidification structure. This study simulated the solidification process of the continuous casting round billets of oil casing steel using a cellular automaton–finite element (CAFE) model. According to the simulation results, at a superheat degree of 20–35 K, a casting speed of 1.9–2.1 m/min, and a secondary cooling specific water flow of 0.34–0.45 L/Kg, the solidification structure had a relatively high equiaxed crystal ratio and small average grain radius. Guided by the simulation results, this paper establishes optimal process schemes for producing 26CrMoVTiB steel round billets, comparatively analyzes the equiaxed crystal ratio and central shrinkage of round billets produced according to these schemes, and defines the optimal continuous casting process conditions, which are: superheat degree = 25 K, casting speed = 2.1 m/min, and specific water flow = 0.35 L/Kg. When adopting these process parameters, the 26CrMoVTiB steel round billets demonstrate a tiny central shrinkage and an equiaxed crystal ratio of 45.2%.

Keywords: oil casing steel; 26CrMoVTiB; cellular automaton–finite element model; continuous casting process; optimal process schemes

1. Introduction

Oil casing steel is an important metallic material used in the mining of petroleum and natural gas, mainly to support shaft walls and sustain shaft operations [1]. Because of its special application environment and the complicated underground stress states, it must meet extremely high quality requirements. In case of failure during service, it may cause reduction of output, abandonment of a shaft, or even jeopardize the safety of underground workers.

Currently, in most cases, continuous casting round billets are adopted for the production of oil casing steel. The production process, casting speed, superheat degree, secondary cooling intensity, and other process conditions directly influence the solidification structure of continuous casting round billets and further affect the mechanical properties and corrosion resistance of oil casing steel. In this sense, seeking a continuous casting process characterized by higher equiaxed crystal ratio, less composition segregation, and less internal shrinkage constitutes an important prerequisite for producing high-quality oil casting steel and providing a safe production environment in petroleum and natural gas mining. Numerical simulations of metallurgical processes offer an economical and ideal method for studying the solidification phenomenon in continuous casting [2,3]. More specifically, the cellular automaton–finite element (CAFE) model, by virtue of its explicit physical mechanism,

high simulation precision, and other advantages, has been widely applied in the simulation of solidification structure [4–8]. Based on the CAFE model, the simulation of solidification structure provides powerful theoretical support and practical guidance for optimizing the process of continuous casting slabs [9,10], square billets [11–13], round billets [14–17], and other types of steel.

In this paper, after the CAFE model was adopted, a numerical simulation study on the temperature field, solidification behavior, and organization structure of oil casing steel (26CrMoVTiB) round billets in the continuous casting process was conducted. A coupling model for simulating macroscopic heat transfer and microstructure (heterogeneous nucleation, dendritic growth, and solute diffusion) was established, and the influence of casting speed, superheat degree, secondary cooling intensity, and other process conditions on the solidification structure were analyzed. Guided by the simulation results, the continuous casting process scheme of oil casing steel round billets was optimized, the equiaxed crystal ratios of the cast billets were increased, and their quality defects, such as crack and low toughness, were reduced. Finally, through industrial trial production, the quality of round billets produced according to the optimized schemes was comparatively analyzed, and the optimal production process conditions were defined, thus offering theoretical support in the production of high-quality oil casing steel.

2. Methods

2.1. Mathematical Model

The continuous casting process is a very complicated, high-temperature, physical process. The heat transfer differential equation for the continuous casting billet process, coupled with boundary conditions, is highly complex; therefore, the numerical simulation process needs to make some reasonable assumptions on the concrete continuous casting process. A simplified heat transfer differential equation can facilitate the solution of the mathematical model of solidification. Many researchers use these assumptions to establish mathematical models [18–20] which facilitate fast simulation, save computational resources, and do not affect the simulation accuracy. The following assumptions were made: (1) the heat transfer in the moving direction of cast billets was neglected; (2) the liquid level temperature of the molten steel in the crystallizer was equated to the casting temperature of the tundish; (3) the influence of molten steel on the erosion fluctuation of the crystallizer during electromagnetic stirring, crystallizer vibration, and casting was neglected; (4) the influence of molten steel flow on the heat transfer inside the molten steel was neglected; (5) in the secondary cooling zone of continuous casting, the surface cooling of the round billets was uniform in the same cooling zone; a comprehensive coefficient of thermal conductivity was adopted to express the contact heat transfer and surface radiation between the round billet and the back-up roll; (6) latent heat was treated according to the equivalent specific heat method; (7) the density of each phase was set as a constant [21].

The numerical calculation was performed according to the moving boundary method [22]. The 2D thermal conductivity control equation [23] of the macroscopic temperature field is defined as:

$$\rho C_p \frac{\partial T}{\partial t} = \frac{\partial}{\partial x}\left(\lambda \frac{\partial T}{\partial x}\right) + \frac{\partial}{\partial y}\left(\lambda \frac{\partial T}{\partial y}\right) + \rho \Delta H \frac{\partial f_s}{\partial t} \quad (1)$$

where ρ denotes density, C_p is the thermal capacity, T is the temperature, λ is the thermal conductivity, ΔH is the solidification latent heat, and f_s is the solidification rate.

The CA method was adopted to simulate grain growth. Due to the relatively significant nucleation difference between the inside and the surface of cast billets, two groups of data were used to characterize the internal and surface nucleation behaviors in the simulation process. Considering the preferred orientation of grains during growth, the <1 0 0> grain class of preferentially growing grains was

adopted as the object of study. The continuous equation of heterogeneous nucleation and the calculation formula of grain density [7] are respectively expressed by:

$$\frac{dn}{d(\Delta T)} = \frac{n_{max}}{\sqrt{2\pi}\Delta T_\sigma} exp\left[-\frac{1}{2}\left(\frac{\Delta T - \Delta T_N}{\Delta T_\sigma}\right)\right] \quad (2)$$

$$n\Delta T = \int_0^{\Delta T} \frac{dn}{d\Delta T} d\,(\Delta T) \quad (3)$$

where ΔT_N denotes the average nucleation supercooling degree, ΔT_σ is the standard deviation of the nucleation supercooling degree, and n_{max} is the compliance of maximum nucleation density with normal distribution.

The dendritic tip growth rate in the solidification process can be expressed by a fitted Dendrite growth kinetics model (KGT model) [24]:

$$V(\Delta T) = a_1(\Delta T)^2 + a_2(\Delta T)^3 \quad (4)$$

where the fitting coefficients are $a_1 = 0$ and $a_2 = 7.511 \times 10^{-6}$ m·s^{-1}·K^{-3}.

In order to reveal the crystal growth laws of solidification structure in the continuous casting process, an interpolation coefficient was defined between FE grid and CA grid nodes. The two methods were coupled in one model to predict the functional relationship of grain growth variation with heat field and latent heat release. In the simulation process, a wafer, 178 mm in diameter and 3 mm in thickness, was meshed using 19,373 finite-element nodes and 89,559 cells (Figure 1).

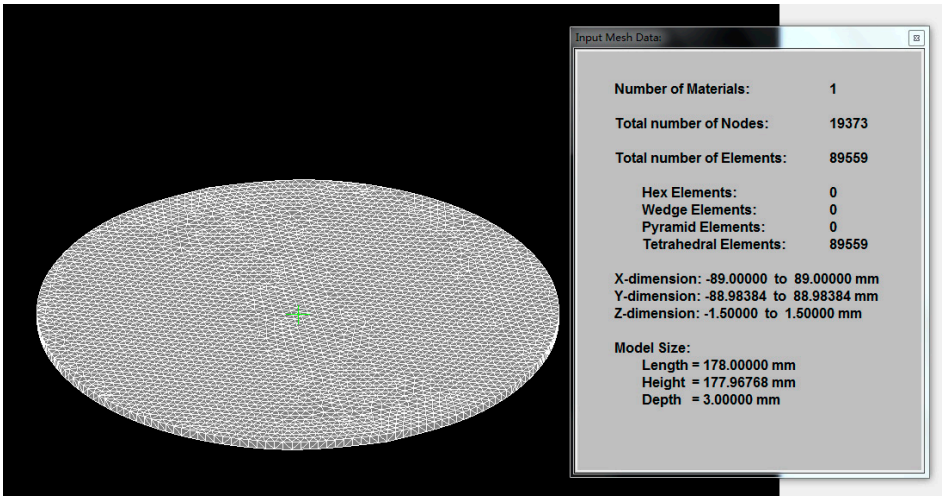

Figure 1. Simulated physical model.

2.2. Thermo-Physical Properties

Table 1 lists the contents and physical parameters of the elements in the 26CrMoVTiB steel (except for the base metal element Fe).

The changes in density, enthalpy, solid fraction, and thermal conductivity of the 26CrMoVTiB steel with temperature were calculated according to the data listed in Table 1, using the pre-processing module of the ProCast 2018 software(UES (UNIVERSAL ENERGY SYSTEM), Cleveland, OH, USA) (Figure 2).

Table 1. Element contents and physical parameters of 26CrMoVTiB.

Element	Mass Fraction (wt %)	Liquidus Slope in Binary Fe-X System	Partition Coefficient	Self-Diffusion Coefficient (m^2/s)
C	0.255	−84.9	0.23	14.7×10^{-9}
Si	0.25	−17.9	0.65	1.4×10^{-9}
Mn	0.48	−3.3	0.45	1.6×10^{-9}
P	0.01	−32.6	0.09	3.1×10^{-9}
V	0.10	−36.7	0.98	11.0×10^{-9}
S	0.001	−5.1	0.01	0.7×10^{-9}
Cr	0.50	−0.6	0.47	1.6×10^{-9}
Mo	0.75	−5.7	0.80	1.1×10^{-9}

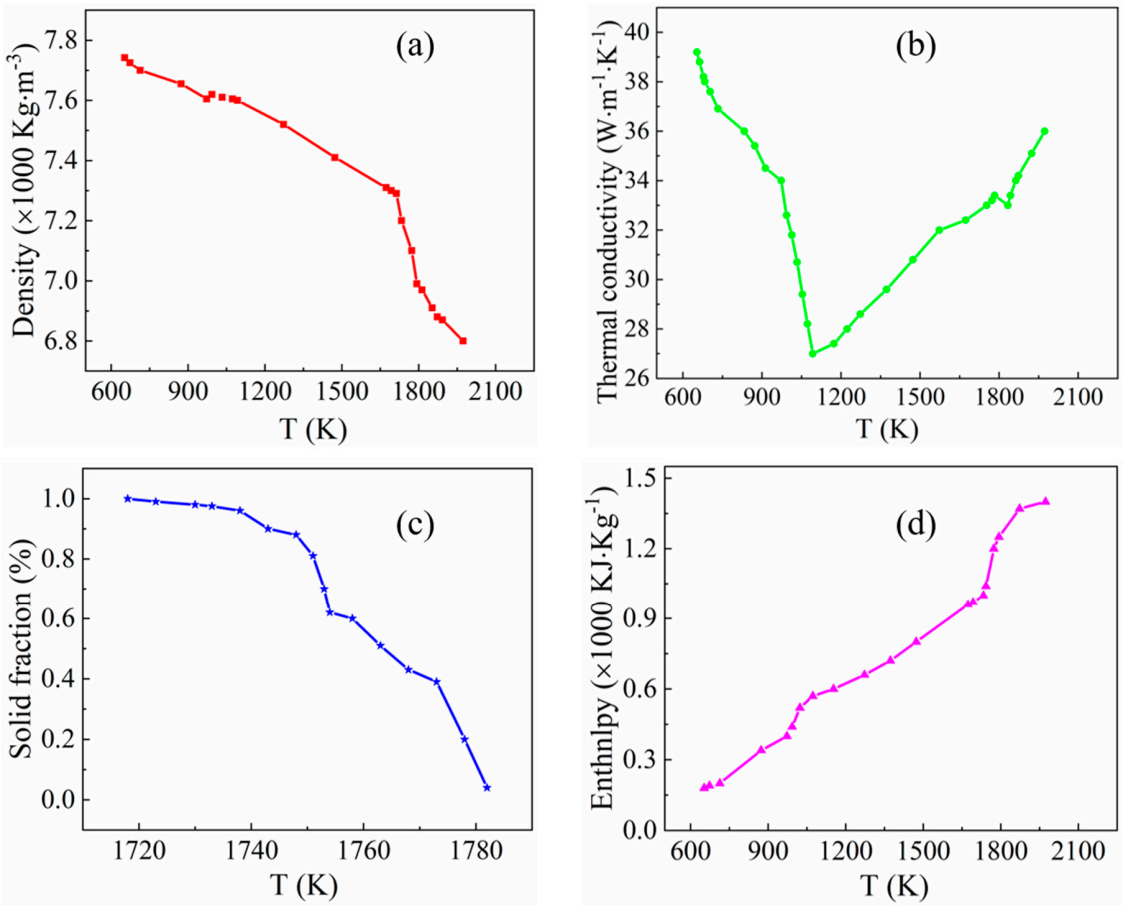

Figure 2. Changes in (**a**) density, (**b**) thermal conductivity, (**c**) solid fraction, and (**d**) enthalpy of the 26CrMoVTiB steel with temperature.

During actual production, the round billet continuous casting machine had a radius of 10 m and a maximum casting speed of 2.3 m/min. Its main process parameters are listed in Table 2.

Table 2. Process parameters of the round billet continuous casting machine.

Parameter	Value
Crystallizer length (mm)	900
Crystallizer water volume (L/min)	1700
Cast billet size (mm)	Φ178
Superheat degree (K)	40
Casting speed (m/min)	1.9
Specific water flow (L/Kg)	0.64
Cooling water ratio in the secondary cooling segment	24:17:16:13

2.3. Model Verification

In order to verify the accuracy of the heat transfer model, an Opps IR P20H1 (Shenzhen oupushi electronic technology co., LTD, Shenzhen, China) infrared thermometer, which can measure temperatures of 650–1800 °C with an accuracy of 0.3%, and spectral reaction times of 0.9–1.7 um and 500 ms, was used to measure the cast billet surface temperature at sites 10.9, 12.5, 13.5, 14.5, 15.5, 16.5, and 19 m away from the meniscus at the actual production site of 26CrMoVTiB steel. The measured temperatures were compared to the temperatures calculated by the model (Figure 3). Clearly, there was a temperature difference of ≤16 K between the simulation results and the measured results, with an error of ≤1.67%. This suggests that the established mathematical model for heat transfer can properly reflect the status of macroscopic heat transfer in the continuous casting process.

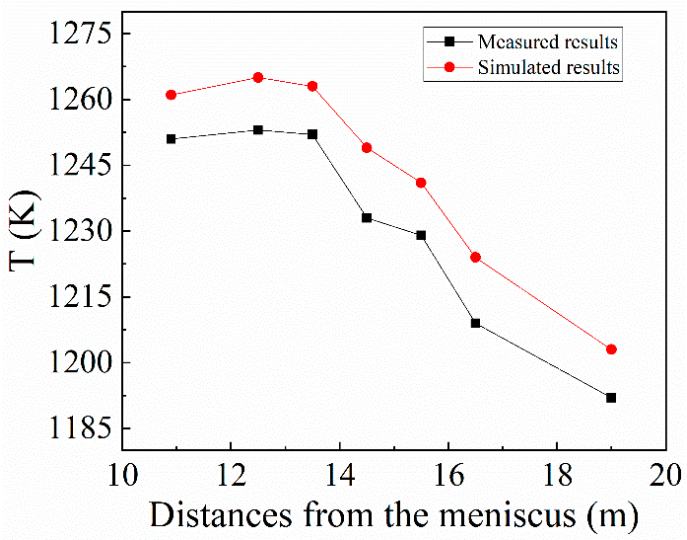

Figure 3. Comparison between the cast billet surface temperature simulation and measured results.

In order to verify the accuracy of the solidification model for cast billets, the simulation results were compared to low-magnification images of continuous cast billets after dendritic corrosion (Figure 4). The equiaxed crystal ratio is the ratio of the area of the equiaxed crystal zone to the cross section area of the billet. Clearly, the simulation and measured results of the central equiaxed crystal ratio of the continuous cast billet were 36.7% and 37.0%, respectively, with a relative error of only 0.3%. This suggests that the established microstructural model can satisfactorily describe the solidification structure of cast billets.

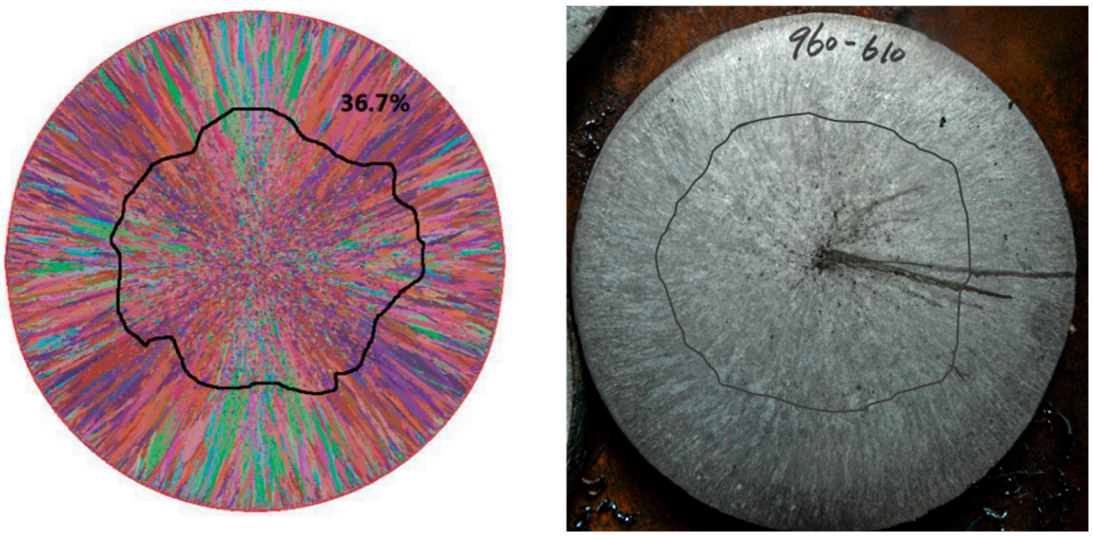

Figure 4. Simulation results and measured results of a continuous casting round billet, where the casting billet diameter is 178 mm on the left side.

2.4. Industrial Trial Production

After analyzing the simulation results, the optimal combination schemes of three process parameters (i.e., superheat degree, casting speed, and secondary cooling intensity) were established. Based on the optimal schemes, the industrial trial production of oil casing steel round billets was carried out. Through observing the low-power images of trial-produced samples, the quality of the round billets was analyzed. Ten cast billet samples from the trial-produced samples of each scheme were randomly selected, and the equiaxed crystal ratios of the cast billets were examined. The average values of 10 groups of samples were used as measurement criteria.

Before observing the low-power image and analyzing the equiaxed crystal ratio of a sample, a planer was used to plane the scratches on the sample surface, followed by buffing with 100-mesh, 240-mesh, and 2000-mesh abrasive papers. Afterwards, a diamond paste with a granularity of w2.5 was used to polish the sample until the coarseness of the surface was below 0.1 μm. Next, the polished surface was subjected to dendritic corrosion by a 4% alcohol–nitric acid solution for 2 min. Deionized water was used to remove the corrosive liquid, and anhydrous alcohol was used for secondary washing, which was followed by drying for later use.

3. Results and Discussion

3.1. Influence of the Superheat Degree on the Solidification Structure

The microstructure simulations were performed under the following conditions: casting speed = 2.0 m/min; secondary cooling of specific water flow = 0.51 L/Kg; superheat degree = 15, 25, 35, and 45 K. The simulation results are presented in Figure 5.

As can be seen in Figure 5a–d, with the increase of the superheat degree, the number of grains in the solidification structure gradually decreased, accompanied by a continuous decline in the central equiaxed crystal ratios of the cast billets. In order to more accurately analyze the influence of the superheat degree on the solidification structure, the simulation results were analyzed to identify changes in the equiaxed crystal ratio (Figure 5e), grain number (Figure 5g), and average grain radius (Figure 5f). As can be seen in Figure 5e, when the superheat degree exceeded 25 K, the equiaxed crystal ratio in the solidification structure decreased significantly. More specifically, when the superheat degree increased from 25 K to 45 K, the central equiaxed crystal ratio of the cast billet decreased from 56% to 44%. Correspondingly, with the increase of the superheat degree, the grain number in the solidification structure (Figure 5f) presented an obvious declining trend, while the average grain radius

(Figure 5g) showed an obvious increasing trend, which was manifested by its increase from 0.5173 mm at 15 K to 0.5893 mm at 45 K.

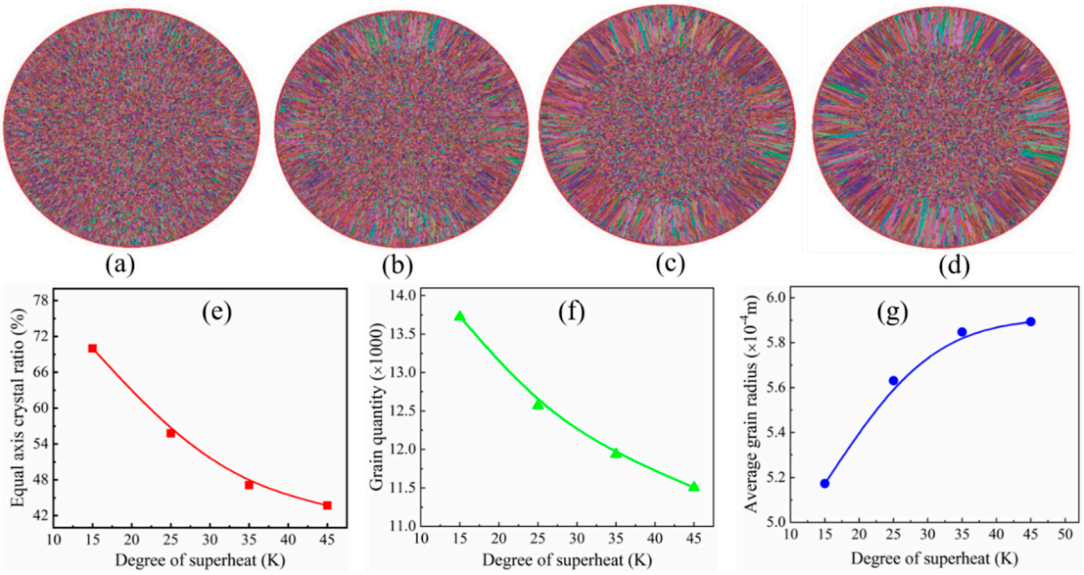

Figure 5. Influence of the superheat degree on the solidification structure (**a**–**d**): solidification structure morphology at superheat degrees of 15, 25, 35, and 45 K, respectively; (**e**–**g**): changes in equiaxed crystal ratio, grain number, and average grain radius with the superheat degree, respectively.

According to the constitutional supercooling theory, in the continuous casting process there is a solute enrichment layer at the solid–liquid interface front. With the decrease of the superheat degree, the temperature gradient in the molten steel decreases, while the constitutional supercooling zone gradually expands, thus forming an equiaxed crystal zone. This zone grows continuously and prevents the growth of columnar crystals inside the continuous cast billets. Thus, when the temperature is low enough, massive heterogeneous nucleation takes place inside the molten steel. As a result of growth under mutual inhibition between crystal nuclei, an as-cast structure consisting of tiny equiaxed crystals is eventually formed. In production practice, when the superheat degree of molten steel becomes excessively low, its castability becomes weaker. For this reason, based on the simulation results, it was reasonable to control the superheat degree of molten steel within the range of 15–35 K, so as to increase the equiaxed crystal ratios of cast billets and improve their internal quality under the premise of guaranteeing the successful casting of molten steel. Considering that an excessively low superheat degree frequently results in the attachment of molten steel to the tundish and causes damage to the industrial production, the optimal superheat degree should be maintained within the range of 20–35 K.

3.2. Influence of the Casting Speed on the Solidification Structure

Figure 6 shows the simulation results of the continuous cast billets made of 26CrMoVTiB steel under the following process conditions: superheat degree = 25 K; secondary cooling water rate = 0.45 L/Kg; casting speed = 1.8, 1.9, 2.1, and 2.3 m/min. As can be seen in Figure 6a–d, as the casting speed changed, no obvious change occurred in the micro-morphology of the solidification structure. According to data statistics, when the casting speed increased from 1.8 to 2.3 m/min, the equiaxed crystal ratio in the solidification structure increased only by about 3% (Figure 6e), the grain number fluctuated at relatively low amplitudes (Figure 6f), and the average grain radius experienced no obvious change, with the difference between its maximum (0.6899 mm) and its minimum value (0.6813 mm) being only 0.086 mm (Figure 6g). This was possibly due to the small fluctuations in casting speed not significantly changing the thermal boundary conditions, and the temperature field distribution of the molten steel changing little during the solidification process. During actual production, in order to ensure that the cast billets have a shell thickness that can sustain their internal molten steel quality and to reduce

breakout accidents, it is necessary to maintain the casting speed at a moderate level. After giving a comprehensive consideration to both simulation results and production practice, it was determined that the optimal casting speed should be set within the range of 1.9–2.1 m/min for the continuous casting of 26CrMoVTiB steel round billets.

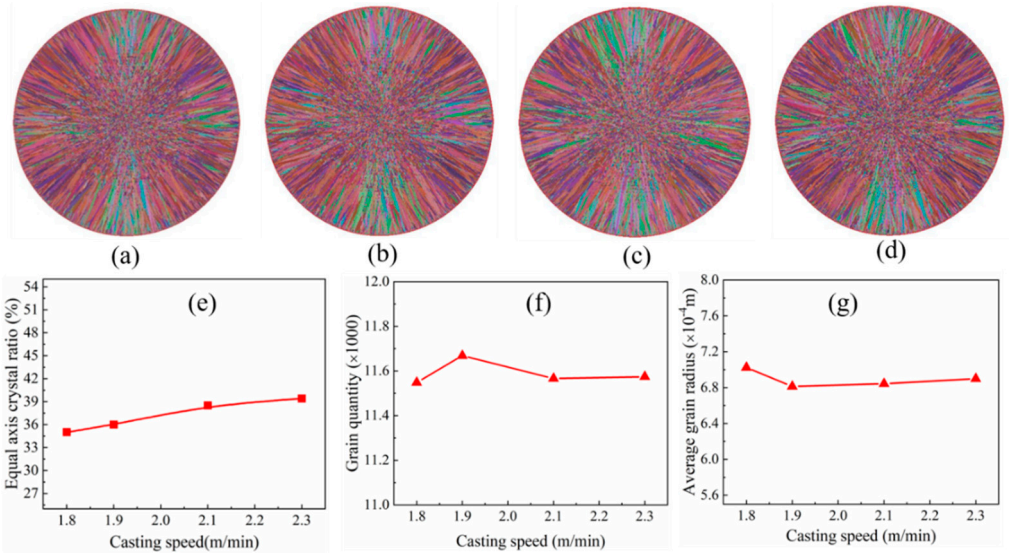

Figure 6. Influence of the casting speed on the solidification structure (**a**–**d**): solidification structure morphology at casting speeds of 1.8, 1.9, 2.1, and 2.3 m/min, respectively; (**e**–**g**): changes of equiaxed crystal ratio, grain number, and average grain radius with casting speed, respectively.

3.3. Influence of the Secondary Cooling Intensity on the Solidification Structure

The secondary cooling distribution system has a great influence on the surface and internal quality of continuous cast billets, and a suitable secondary cooling intensity can effectively inhibit the growth of columnar crystals inside continuous cast billets and avoid the occurrence of serious central shrinkage. The secondary cooling intensity is reflected by, and positively correlated with, the specific water flow. Figure 7 shows the microstructure simulation results of the continuous cast billets made of 26CrMoVTiB steel under the following process conditions: superheat degree = 25 K; casting speed = 1.9 m/min; specific water flow = 0.30, 0.35, 0.45, and 0.51 L/Kg.

As can be seen in Figure 7a–d, as the specific water flow increased, the micro-morphology of the solidification structure changed obviously. When the temperature gradient in the molten steel was low, more crystal nuclei were formed at the solidification front. The mutual inhibition between crystal nuclei lowered the possibility of the occurrence of columnar crystals, helped to expand the central equiaxed crystal zone of the cast billets, and thereby increased the equiaxed crystal ratio. According to data statistics, when the specific water flow increased from 0.30 L/Kg to 0.51 L/Kg, the equiaxed crystal ratio of the cast billets decreased from 43.3% to 39.0% (Figure 7e), the grain number reduced from 12,188 to 11,975 (Figure 7f), and the average grain radius increased from 0.4140 mm to 0.4398 mm (Figure 7g). According to the simulation results of Figure 7, in order to increase the equiaxed crystal ratio of a cast billet, the secondary cooling system in the production process should adopt a slow cooling process, that is, a low specific water flow should be selected during secondary cooling distribution. However, given that an excessively low specific water flow in production practice can very easily cause surface cracks on the cast billets and lower their quality, it is necessary to seek an optimal secondary cooling specific water flow within the range of 0.35–0.45 L/Kg.

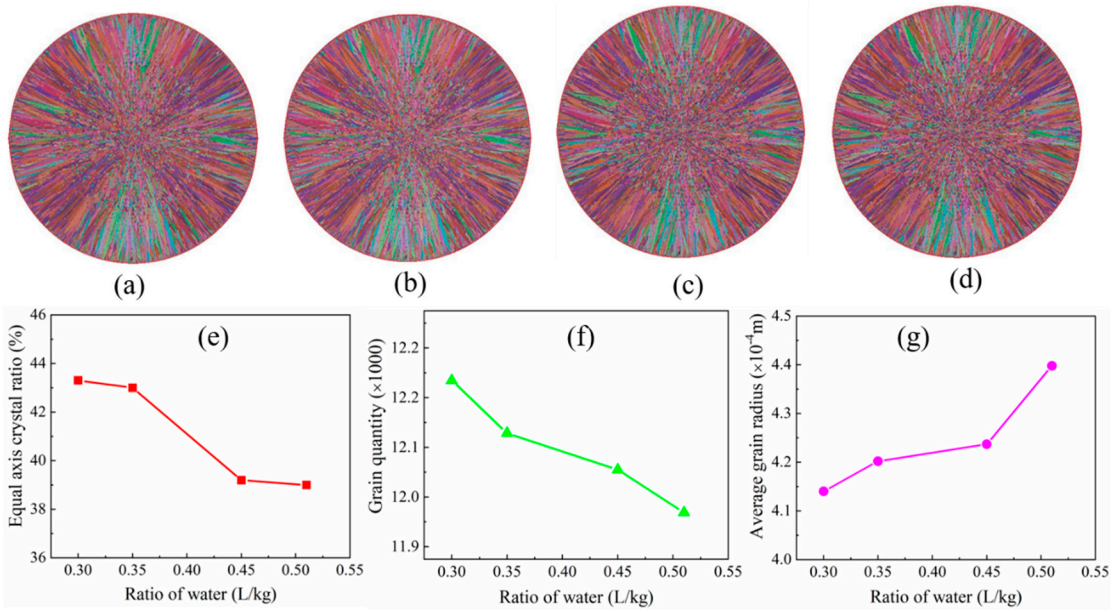

Figure 7. Influence of the casting speed on the solidification structure (**a**–**d**): solidification structure morphology at specific water flows of 0.30, 0.35, 0.45, and 0.51 L/Kg, respectively; (**e**–**g**): changes of equiaxed crystal ratio, grain number, and average grain radius with specific water flow, respectively.

3.4. Industrial Trial Production Results

Through simulating the solidification process of oil casing steel round billets, it can be seen that properly lowering the superheat degree and specific water flow helped to increase the grain number, reduce the average grain radius, and increase the equiaxed crystal ratio, which further facilitated the improvement of the product quality of oil casing steel. In this paper, by combining the simulation results with production experience, three optimal schemes for producing oil casing steel round billets were established. The process parameters are listed in Table 3.

Table 3. Design scheme of continuous casting process parameters.

Continuous Casting Process Plan	Superheat Degree (K)	Casting Speed (m/min)	Specific Water Flow (L/Kg)
Original process	40	1.9	0.64
Scheme I	30	2.0	0.40
Scheme II	25	2.1	0.35
Scheme III	35	1.9	0.45

Figure 8 shows low-power images of round billet samples produced according to the original process conditions and the three optimal schemes. Clearly, at the center of the round billet sample produced according to the original process conditions, there was an obvious shrinkage phenomenon. In contrast, the round billet samples produced according to the optimized process parameters demonstrated a significant improvement in central shrinkage. In particular, the central shrinkage on the round billet samples produced according to schemes II and III was extremely small.

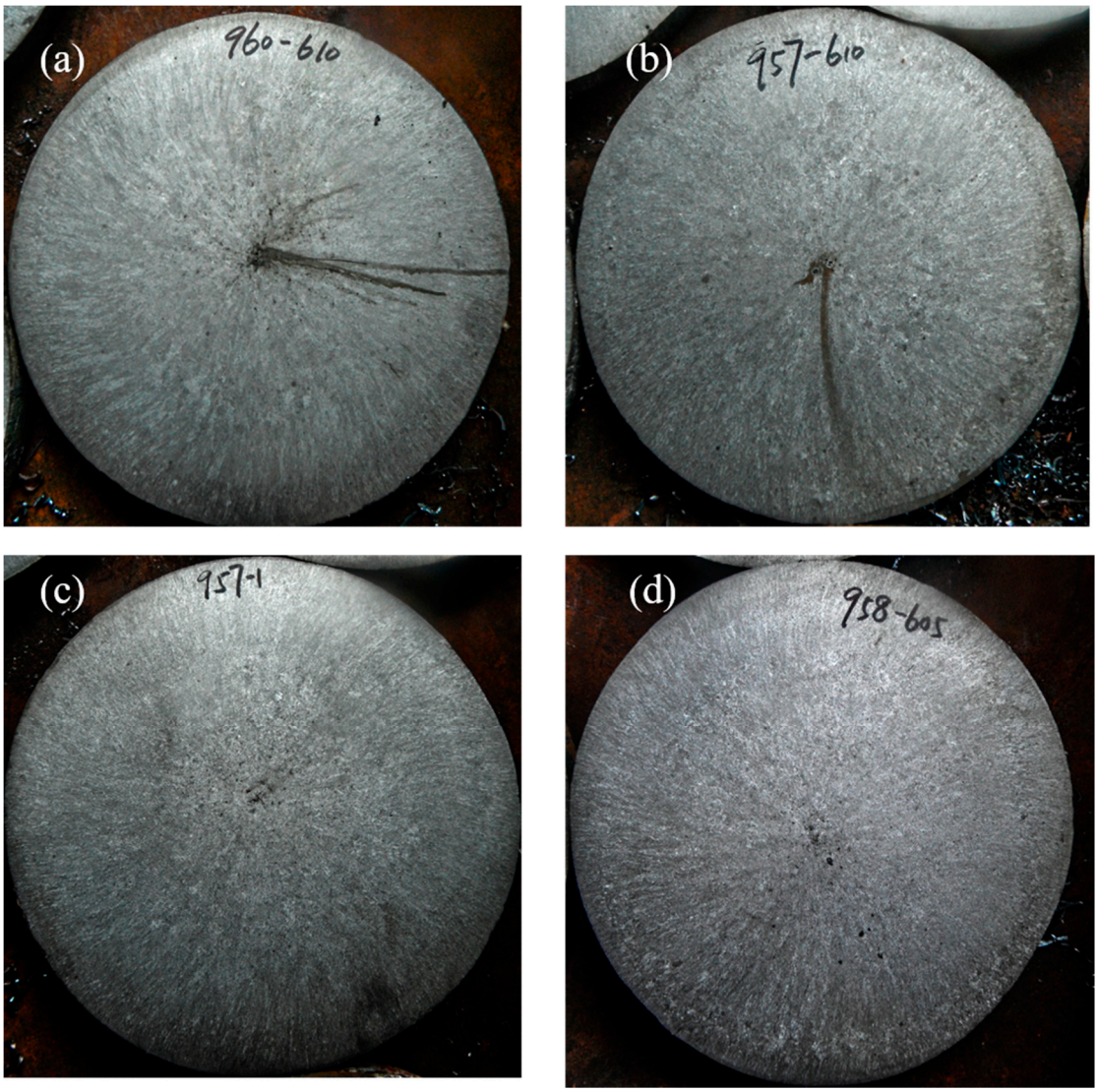

Figure 8. Low-power images of round billet samples produced according to the (**a**) original process, (**b**) scheme I, (**c**) scheme II, and (**d**) scheme III, where the casting billet diameter is 178 mm.

In order to better understand the equiaxed crystal ratios of the cast billet samples produced according to the optimal schemes, a critical index that has a great bearing on steel quality was employed. Ten cast billet samples from the trial production samples of each scheme were randomly selected, and their equiaxed crystal ratios were analyzed (Table 4).

Table 4. Low-power test results under the equiaxed crystal ratios of cast billet samples produced according to different schemes.

Scheme	Original Process	I	II	III
Equiaxed crystal ratio (%)	37.0	41.8	45.2	39.6
Improvement (%)	0	4.8	8.2	2.6

As can be seen in Table 4, all cast billet samples produced according to the optimized process parameters experienced some increase in the equiaxed crystal ratio. In particular, the equiaxed crystal ratio of the cast billet sample produced according to scheme II (superheat degree = 25 K; casting speed = 2.1 m/min; specific water flow = 0.35 L/Kg) experienced the greatest increase, and its equiaxed crystal ratio rose from 37.0% to 45.2%. In this case, the central shrinkage of the cast billet was also

extremely small (Figure 8c). The significant increase in the equiaxed crystal ratio and the obvious reduction in central shrinkage indicated that the oil casing steel produced according to this process experienced an obvious quality improvement.

4. Conclusions

In this study, the process parameter ranges for optimized production schemes were acquired by simulating the solidification structure of steel billets in the continuous casting process, and then the optimal schemes for improving steel billet quality were established according to production experience. Relying on industrial trial production, the optimal continuous casting process parameters for producing 26CrMoVTiB steel round billets were successfully obtained.

The simulating results showed that both the superheat degree and the secondary cooling intensity exerted some influence on the equiaxed crystal ratio, grain number, and average grain radius of 26CrMoVTiB steel and greatly affected its solidification structure in round billet continuous casting. However, the casting speed had no significant influence on the above quality parameters. Through industrial trial production, the optimal continuous casting process parameters of 26CrMoVTiB steel round billets were acquired, as follows: superheat degree = 25 K, casting speed = 2.1 m/min, and specific water flow = 0.35 L/Kg. When these process parameters were adopted, the 26CrMoVTiB steel round billets demonstrated a small central shrinkage and an equiaxed crystal ratio of 45.2%.

The simulation results guided the establishment of the optimal schemes, reduced the blindness of scheme preparation, reduced the workload of actual tests to a great extent, and decreased the test cost. This can be seen as an effective case of simulating and guiding the production practice.

Author Contributions: Conceptualization, Y.Z. and K.P.; methodology, D.W.; software, Y.Z. and D.W.; formal analysis, Y.Z.; writing—original draft preparation, Y.Z.; writing—review and editing, K.P.; project administration, K.P.

Funding: This research was funded by The Fundamental Research Funds for the Central Universities, China, grant number N171603015; The National Key Research Program during the 13th Five-Year Plan Period of China, grant number 2017YFB0304200 and The Liaoning Shihua University Foundation, China, grant number 2018XJJ-001.

Conflicts of Interest: The authors declare no conflict of interest.

References

1. Li, H.-Y.; Li, Y.-H.; Wei, D.-D.; Liu, J.-J.; Wang, X.-F. Constitutive equation to predict elevated temperature flow stress of V150 grade oil casing steel. *Mater. Sci. Eng. A* **2011**, *530*, 367–372. [CrossRef]
2. Thomas, B.G. Modeling of the continuous casting of steel-past, present, and future. *Met. Mater. Trans. B* **2002**, *33*, 795–812. [CrossRef]
3. Mauder, T.; Stetina, J. High Quality Steel Casting by Using Advanced Mathematical Methods. *Metals* **2018**, *8*, 1019. [CrossRef]
4. Zhang, Q.; Xue, H.; Tang, Q.; Pan, S.; Rettenmayr, M.; Zhu, M. Microstructural evolution during temperature gradient zone melting: Cellular automaton simulation and experiment. *Comput. Mater. Sci.* **2018**, *146*, 204–212. [CrossRef]
5. Luo, S.; Zhu, M.Y. A two-dimensional model for the quantitative simulation of the dendritic growth with cellular automaton method. *Comput. Mater. Sci.* **2013**, *71*, 10–18. [CrossRef]
6. Gandin, C.-A.; Desbiolles, J.-L.; Rappaz, M.; Thevoz, P. A three-dimensional cellular automation-finite element model for the prediction of solidification grain structures. *Metall. Mater. Trans. A* **1999**, *30*, 3153–3165. [CrossRef]
7. Thévoz, P.; Desbiolles, J.L.; Rappaz, M. Modeling of equiaxed microstructure formation in casting. *Metall. Trans. A* **1989**, *20*, 311–322. [CrossRef]
8. Wang, C.Y.; Beckermann, C. Prediction of Columnar to Equiaxed Transition during Diffusion-Controlled Dendritic Alloy Solidification. *Metall. Mater. Trans. A* **1994**, *25*, 1081–1093. [CrossRef]
9. Bai, L.; Wang, B.; Zhong, H.; Ni, J.; Zhai, Q.; Zhang, J. Experimental and Numerical Simulations of the Solidification Process in Continuous Casting of Slab. *Metals* **2016**, *6*, 53. [CrossRef]

10. Chen, S.; Chen, J. Micromodel of Simulation on Twin-Roll Continuous Casting Thin Strip Solidification Structure. *Rare Metall. Mater. Eng.* **2013**, *1*, 14–18.
11. Fang, Q.; Ni, H.; Zhang, H.; Wang, B.; Liu, C. Numerical Study on Solidification Behavior and Structure of Continuously Cast U71Mn Steel. *Metals* **2017**, *7*, 483. [CrossRef]
12. Zhu, H.-C.; Jiang, Z.-H.; Li, H.-B.; Zhu, J.-H.; Feng, H.; Zhang, S.-C.; Zhang, B.-B.; Wang, P.-B.; Liu, G.-H. Effect of Solidification Pressure on Compactness Degree of 19Cr14Mn0.9N High Nitrogen Steel Using CAFE Method. *Steel Res. Int.* **2017**, *88*, 1600509. [CrossRef]
13. Zhai, Y.; Ma, B.; Li, Y.; Jiang, Z. Analysis of 13Cr bloom solidification structure using CA-FE model. *J. Cent. South Univ.* **2016**, *23*, 10–17. [CrossRef]
14. Hou, Z.; Cheng, G.; Jiang, F.; Qian, G. Compactness Degree of Longitudinal Section of Outer Columnar Grain Zone in Continuous Casting Billet Using Cellular Automaton-Finite Element Method. *ISIJ Int.* **2013**, *53*, 655–664. [CrossRef]
15. Cailiang, J.; Zhigang, X.; Ying, W.; Wanjun, W. Simulation on solidification structure of 72A tire cord steel billet using CAFE method. *China Foundry* **2012**, *9*, 53–59.
16. Hou, Z.; Jiang, F.; Cheng, G. Solidification Structure and Compactness Degree of Central Equiaxed Grain Zone in Continuous Casting Billet Using Cellular Automaton-Finite Element Method. *ISIJ Int.* **2012**, *52*, 1301–1309. [CrossRef]
17. Luo, Y.Z.; Zhang, J.M.; Wei, X.D.; Xiao, C.; Hu, Z.F.; Yuan, Y.Y.; Chen, S.D. Numerical simulation of solidification structure of high carbon SWRH77B billet based on the CAFE method. *Ironmak. Steelmak.* **2012**, *39*, 26–30. [CrossRef]
18. Louhenkilpi, S.; Laitinen, E.; Nieminen, R. Real-time simulation of heat transfer in continuous casting. *Metall. Trans. B* **1993**, *24*, 685–693. [CrossRef]
19. Thomas, B.G.; Najjar, F.M. Finite element modelling of turbulent fluid flow and heat transfer in continuous casting. *Appl. Math. Model.* **1991**, *15*, 226–243. [CrossRef]
20. Tieu, A.K.; Kim, I.S. Simulation of the continuous casting process by a mathematical model. *Int. J. Mech. Sci.* **1997**, *39*, 185–192. [CrossRef]
21. Li, C.; Thomas, B.G. Thermomechanical finite-element model of shell behavior in continuous casting of steel. *Met. Mater. Trans. B* **2004**, *35*, 1151–1172. [CrossRef]
22. Han, H.N.; Lee, J.-E.; Yeo, T.; Won, Y.M.; Kim, K.; Oh, K.H.; Yoon, J.-K. A Finite Element Model for 2-Dimensional Slice of Cast Strand. *ISIJ Int.* **1999**, *39*, 445–454. [CrossRef]
23. Choudhary, S.K.; Mazumdar, D. Mathematical Modelling of Transport Phenomena in Continuous Casting of Steel. *ISIJ Int.* **1994**, *34*, 584–592. [CrossRef]
24. Kurz, W.; Giovanola, B.; Trivedi, R.K. Theory of microstructural development during rapid solidification. *Acta Metall.* **1986**, *5*, 823–830. [CrossRef]